ACS OMEGA

Open Access

http://pubs.acs.org/journal/acsodf

Article

Tannic Acid-Functionalized Silver Nanoparticles as Colorimetric Probe for the Simultaneous and Sensitive Detection of Aluminum(III) and Fluoride Ions

Terefe Tafese Bezuneh,* Natinael Mekonnen Ofgea, Solomon Simie Tessema, and Fuad Abduro Bushira

Cite This: *ACS Omega* 2023, 8, 37293−37301

Read Online

ACCESS | Metrics & More | Article Recommendations | Supporting Information

ABSTRACT: In this study, we employed tannic acid (TA)-functionalized silver nanoparticles (TA@AgNPs) as colorimetric probe for the simultaneous and sensitive detection of Al(III) and F^- ions. The proposed sensor was based on the aggregation and anti-aggregation effects of target Al(III) and F^- ions on TA@AgNPs, respectively. Because of the strong coordination bond between Al(III) ions and TA, the addition of Al(III) ions to TA@AgNPs could cause aggregation and, hence, result in a significant change in the absorption and color of the test solution. Interestingly, in the presence of F^- ions, the aggregation effect of Al(III) ions on TA@AgNPs can be effectively prevented. The extent of aggregation and anti-aggregation effects was concentration-dependent and can be used for the quantitative detection of Al(III) and F^- ions. The as-proposed sensor presented the sensitive detection of Al(III) and F ions with limits of detection (LOD) of 0.2 and 0.19 μM, respectively. In addition, the proposed sensor showed excellent applicability for the detection of Al(III) and F^- ions in real water samples. Moreover, the sensing strategy offered a simple, rapid, and sensitive detection procedure and could be used as a potential alternative to conventional methods, which usually involve sophisticated instruments, complicated processes, and a long detection time.

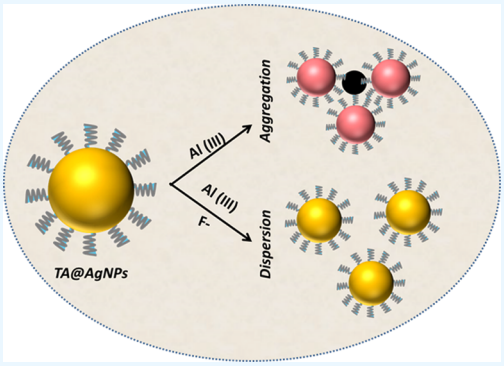

INTRODUCTION

Colorimetric sensors, which are based on detectable color changes, have been widely used for the detection of various target analytes. In this regard, noble metal nanoparticles such as silver nanoparticles (AgNPs) and gold nanoparticles (AuNPs) have been extensively employed as efficient color signal generators in the fabrication of various colorimetric sensors.[1−6] AuNPs and AgNPs have attracted significant research interest in the design of colorimetric sensors because of their easy probe preparation, fast response, unique optical properties (surface plasmon resonance (SPR)), and flexibility in synthesis approaches. To date, a significant number of AgNP- and AuNP-based colorimetric probes for the detection of metal ions,[7−9] herbicides,[10,11] and proteins[9,12] have been reported.

In designing AgNP- and AuNP-based colorimetric sensors, aggregation and anti-aggregation sensing mechanisms are the most commonly employed sensing strategies. Aggregation-based sensing strategies are based on the target-triggered aggregation of nanoparticles, which eventually results in a change in optical properties (i.e., color and SPR).[13−17] In the anti-aggregation sensing mechanism, a non-target linker substance (i.e., molecule, ligands, or ions) induces aggregation of the nanoparticles.[18,19] However, due to strong physico-chemical interactions (e.g., electrostatic, hydrogen bonding, and complexation) between the target analyte and the linker substance, the aggregation of the nanoparticle can be reversed and/or inhibited.[20] The AgNP- and AuNP-based aggregation and anti-aggregation sensors present several interesting features. For instance, the aggregation and/or dispersion phenomenon displays a visible color change that can be observed by the naked eye, and hence, qualitative and quantitative analysis could be performed without the need for sophisticated instruments.[19,21] In addition, the surface chemistry of AuNPs and AgNPs enables one to choose from a variety of surface-functionalizing ligands and hence develop a probe with improved stability, sensitivity, and selectivity. Also, due to their high extinction coefficients, in general, AgNP- and AuNP-based colorimetric assays show higher sensitivity compared to conventional biochemical detection assays.[22,23]

Aluminum, the third most abundant element on the earth's crust, is widely used in the preparation of various cooking utensils, pharmaceutical products, cosmetics, electric wires, electronic devices, and water purifications.[24−26] This widespread use of aluminum could pave the way for its high

Received: July 15, 2023
Accepted: September 15, 2023
Published: September 29, 2023

Scheme 1. Schematic Representation of the Sensing Mechanism for Al(III) and F^- Ions Detection

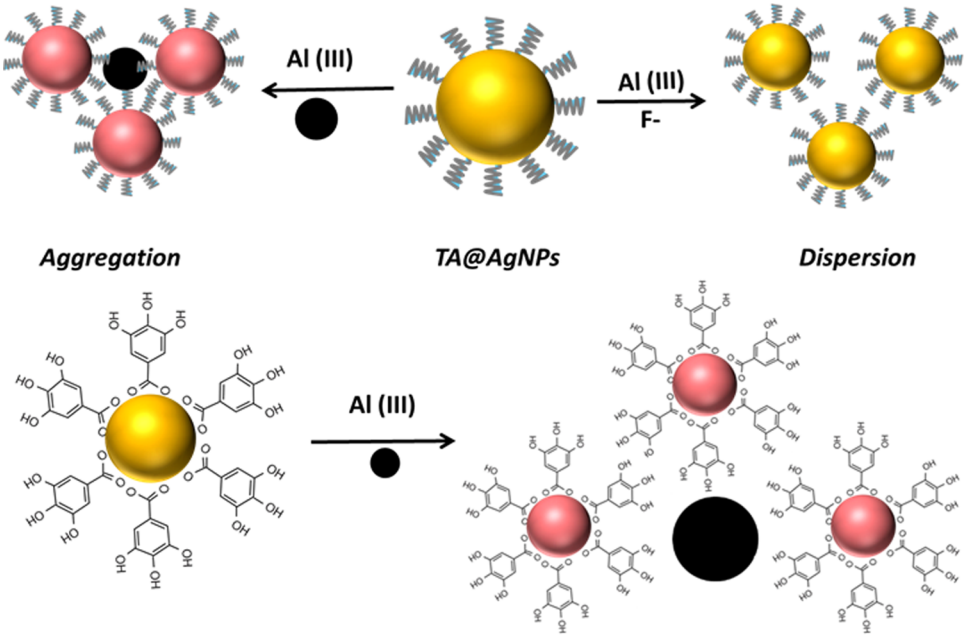

exposure to biological systems, which in turn could result in many toxic effects, including Alzheimer's and Parkinson's disease, dementia, kidney damage, or even cancer.[27−31] Hence, it is important to selectively and sensitively detect aluminum (Al(III)) ions. In addition, the sensitive and selective detection of fluoride ions is of significant interest, as excessive exposure to this ion could cause various health problems. For instance, fluoride intake above a permissible level can cause various diseases, including neurological disorders, fluorosis, urolithiasis, osteoporosis, and metabolic dysfunctions.[32−34] Because of its toxic effects, the World Health Organization (WHO) set the maximum permissible level of fluoride ion in drinking water as 1.50 mg/L.

To date, various AuNP- and AgNP-based colorimetric sensors for the detection of Al(III) and F^- ions have been reported. In these reports, AgNPs and AuNPs functionalized with various ligands such as diaminodiphenyl sulfone,[35] xylenol orange,[36] thioglucose,[37] 11-mercaptoundecanoic acid,[38] polyacrylate,[39] and ascorbic acid[40] were employed as probes. Although these probes showed excellent detection performance, they are not without limitations. For instance, most of these sensors showed low sensitivity, required a longer detection time, and suffered from interferences. In addition, some of these methods involved a complex and tedious probe synthesis procedure and also utilized expensive ligands. Moreover, as surface-functionalizing agents play a key role in determining the sensitivity and selectivity of probes, it is important to search for a new functionalizing ligand with improved performance. Based on these observations, in our present study, we proposed a simple, sensitive, and selective probe for the simultaneous detection of Al(III) and F^- ions. In the detection procedure, tannic acid (TA)-functionalized AgNPs were used as the detection probe. As far as we are concerned, although TA is reported widely as a reducing agent in the synthesis of AgNPs,[41−43] it has not been reported in the colorimetric detection of Al(III) or F^- ions. Moreover, the ligand we employed (TA) is abundant in nature, easily accessible, and biocompatible.

Herein, we employ TA@AgNPs as a colorimetric sensor for the simultaneous and sensitive detection of Al(III) and F^- ions (Scheme 1). The as-proposed sensor can sensitively and selectively detect Al(III) and F^- ions based on their aggregation and anti-aggregation effects, respectively. In the detection system, because of the strong chelation between Al(III) and TA, the addition of target Al(III) ions can cause the aggregation of TA@AgNPs. However, in the presence of F^- ions, the aggregation effect of Al(III) ions on TA@AgNPs can be prevented. The extent of aggregation and anti-aggregation was concentration-dependent, and hence, it can be used to quantitatively detect Al(III) and F^- ions. The proposed detection procedure demonstrated a fast response with excellent sensitivity and selectivity for the detection of Al(III) and F^- ions. Moreover, the sensor could also be used for the visual detection of Al(III) and F^- ions in real samples.

EXPERIMENTAL SECTION

Materials and Reagents. Silver nitrate ($AgNO_3$) was provided by the Chemistry Reagent Factory (Chengdu, China). Aluminum chloride ($AlCl_3$), tannic acid ($C_{76}H_{52}O_{46}$), and trisodium citrate ($Na_3C_6H_5O_7$) were purchased from Sigma-Aldrich. Sodium fluoride (NaF) was obtained from Guangdong Guanghua Sci. Tech. Co. Ltd. EDTA was provided by Yuan Ye Bio-Technology Co. Ltd. (Shanghai, China). Nitrates, chlorides, and sulfates were used to prepare various metal ion solutions, while solutions of anions were prepared from sodium or potassium salts. Before use, all glassware was soaked in HCl solution, carefully washed, and rinsed using distilled water. All chemicals and reagents were of analytical grade and used as provided.

Instruments. Absorption spectra were collected using an ultraviolet−visible (UV−vis) spectrophotometer (Analytik Jena, Jena, Germany). The size and shape of TA@AgNPs were analyzed by transmission electron microscopy (TEM) (Philips Tecnai F20). ζ-potential measurements were performed using a ZetaSizer (Malvern Instruments, U.K.). A Bruker infrared Vertex 70 interferometer was employed to

https://doi.org/10.1021/acsomega.3c05092
ACS Omega 2023, 8, 37293−37301

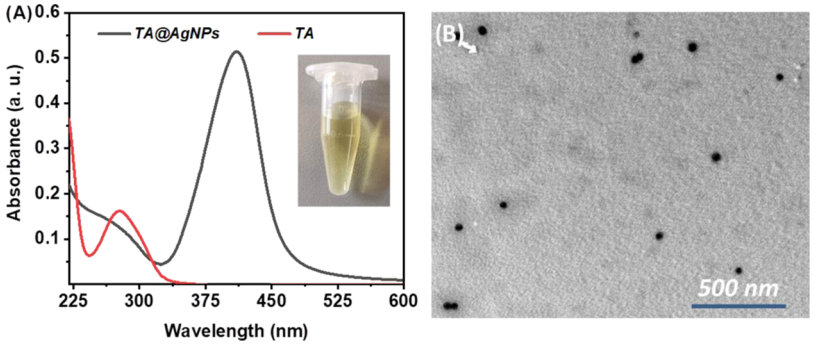

Figure 1. (A) UV−vis absorption spectra and (B) TEM image of TA@AgNPs.

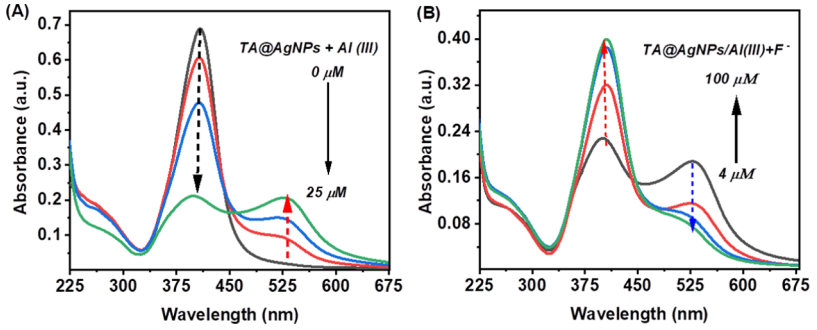

Figure 2. UV−vis absorption responses of TA@AgNPs (A) with various concentrations of Al(III) ions and (B) with 30 μM Al(III) and various concentrations of F^- ions.

perform Fourier-transform infrared (FT-IR) spectroscopic analysis

Synthesis of TA@AgNPs. TA@AgNPs were prepared using TA as a reducing and capping agent toward silver ions following a procedure reported elsewhere.[44−46] In a typical procedure, in a three-neck round-bottom flask, 50 mL of an aqueous solution of 0.1 mM TA and 5 mM sodium citrate was heated with a heating mantle. After heating for about 15 min (under vigorous stirring), 1 mL of 0.25 mM $AgNO_3$ was injected and heating was continued for an additional 10 min. Then, the as-synthesized yellow colloid (TA@AgNPs) was cooled to room temperature, centrifuged at 12,000 rpm for 30 min, and redispersed in double-distilled water. The product was stored at 4 °C until it was required for further experiments.

Detection of Al(III) and F^- Ions. In a 2 mL calibrated flask containing TA@AgNPs, various amounts of Al(III) ions were transferred to obtain the desired concentration. After incubation for about 4 min at room temperature, UV−vis absorption of the test solutions was measured. For the detection of F^- ions, various concentrations of the target ions were added into a solution of TA@AgNPs containing 30 μM of Al(III) ions. Then, the UV−vis absorptions of the test solutions were measured. All measurements were repeated 3 times. The Al(III) and F^- ion concentrations were computed based on the absorption ratio (A_{528}/A_{410}).

RESULTS AND DISCUSSION

Synthesis and Characterization of TA@AgNPs. Figure 1A, shows the UV−vis absorption profile of TA@AgNPs. The as-prepared TA@AgNPs showed a bright-yellow color with a characteristic surface plasmon resonance peak at 410 nm. To reveal the size and morphology of TA@AgNPs, TEM was employed, and the result is presented in Figures 1B and S1. The TEM images showed spherical and well-dispersed TA@AgNPs with a size distribution between 23 and 45 nm and an average size of 33 nm.

Probe Development. The as-proposed sensor was based on the aggregation and anti-aggregation effect of the target analytes on TA@AgNPs. As presented in Figure 2A, the addition of various concentrations of Al(III) ions caused a decrease in the absorption of TA@AgNPs at 410 nm (A_{410}) with the appearance of a new absorption peak at 528 nm (A_{528}) in a concentration-dependent manner. However, in the presence of F^- ions, due to the formation of the water-soluble Al−F complex, aggregation of TA@AgNPs can be suppressed. As a result, as presented in Figure 2B, the absorption peak at 410 nm increased, while the absorption peak at 528 nm decreased with an increasing concentration of F^- ions. The result demonstrated that the aggregation and anti-aggregation effects can be used for the detection of Al(III) and F^- ions. Based on this, the ratio of absorption A_{528}/A_{410} was used to quantitatively determine the concentration of Al(III) and F^- ions.

Optimization of Experimental Variables. As the stability of the probe plays a key role in determining the analytical performance of a given probe, we tested the stability of the proposed sensor at various conditions. Figure S2A shows the effect of pH on the UV−vis absorption of TA@AgNPs. The TA@AgNPs showed aggregation at pH values of 2 and 3. However, TA@AgNPs showed excellent stability in the pH range of 4−12, and hence, the probe could be used in this pH range. Furthermore, the storage stability of the TA@AgNPs probe stored at room temperature in a dark place was tested by recording the UV−vis absorption spectra. As displayed in Figure S2B, the UV−vis absorption spectra of TA@AgNPs measured immediately after synthesis and after storage for 2 months perfectly overlapped, demonstrating its excellent storage stability against chemical dissolution or aggregation.

https://doi.org/10.1021/acsomega.3c05092
ACS Omega 2023, 8, 37293−37301

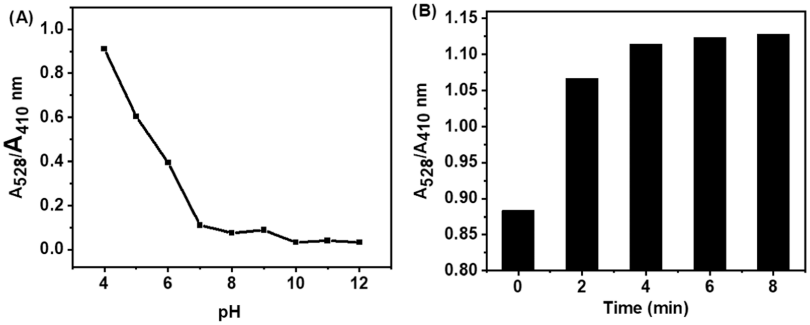

Figure 3. UV−vis absorption response of TA@AgNPs with 25 μM Al(III) at various (A) pH values and (B) incubation times.

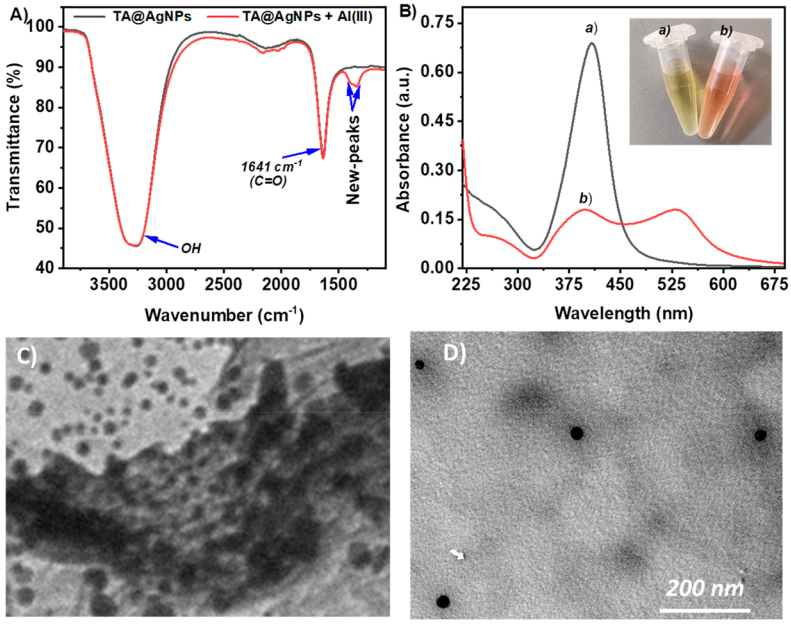

Figure 4. (A) FT-IR spectra of TA@AgNPs in the absence and presence of 100 μM of Al(III) ions. (B) UV−visible absorption spectra of (a) TA@AgNPs and (b) TA@AgNPs with 100 μM Al(III) ions. TEM images of (C) TA@AgNPs with 100 μM Al(III) ions and (D) TA@AgNPs with 100 μM Al(III) and 200 μM F^- ions.

Next, the performance of TA@AgNPs in various solvents such as H_2O, ethanol, and methanol was evaluated. Figure S3 presents the change in the absorption profile of TA@AgNPs (@410 nm) with the addition of various concentrations of Al(III) ions. As presented in the figure, the change in the absorption of TA@AgNPs was significantly higher in aqueous solvents compared to that in ethanol and methanol. Hence, an aqueous solvent was selected as the test medium for successive experiments. Figure S4A presents the effect of pH on the absorption of TA@AgNPs in the presence of Al(III) ions. The TA@AgNPs/Al(III) system showed a pH-dependent absorption spectrum with the maximum degree of aggregation in the pH range of 4−6. The aggregation of TA@AgNPs was further confirmed by a change in the color of the test solution from yellow to light red (Figure S4B). As shown in Figure 3A, a higher absorption ratio (A_{528}/A_{410} nm) was obtained at pH 4, which indicated a higher degree of aggregation at this pH. Hence, this pH was selected as the optimum pH for the next experiments. In addition, as presented in Figure 3B, a higher absorption ratio was obtained at an incubation time of 4 min. Therefore, an incubation time of 4 min was chosen as the optimum time.

Sensing Mechanism for Al(III) and F^- Ions. The proposed detection procedure was based on the aggregation and anti-aggregation effect of target Al(III) and F^- ions. To reveal the sensing mechanism of the detection procedure, various analytical techniques were employed. According to literature results, TA is known for its ability to form a stable complex with Al(III) ions.[47−49] With this in mind, we studied the FT-IR spectra of TA@AgNPs in the presence and absence of Al(III) ions. As presented in Figure 4A, the FT-IR spectra of TA@AgNPs showed two main absorption peaks at 3288 and 1643 cm^{-1} corresponding to hydroxyl and carboxylic functional groups, respectively. However, after the addition of Al(III) ions into TA@AgNPs, new absorption peaks appeared at 1396 and 1338 cm^{-1}. The weak absorption band at 1396 cm^{-1} could be attributed to the interaction of Al(III) ions with carboxylate groups.[50] The new intense absorption band at 1338 cm^{-1} could be related to the interaction of Al(III) ions with the ester groups in TA.[51,52] The above results demonstrated the possible complex formation between Al(III) ions and functional groups in TA. The aggregation of TA@AgNPs with the addition of Al(III) ions further proved the possible coordination interaction. As a result, the absorption profile of TA@AgNPs significantly changed with a decrease in

https://doi.org/10.1021/acsomega.3c05092
ACS Omega 2023, 8, 37293−37301

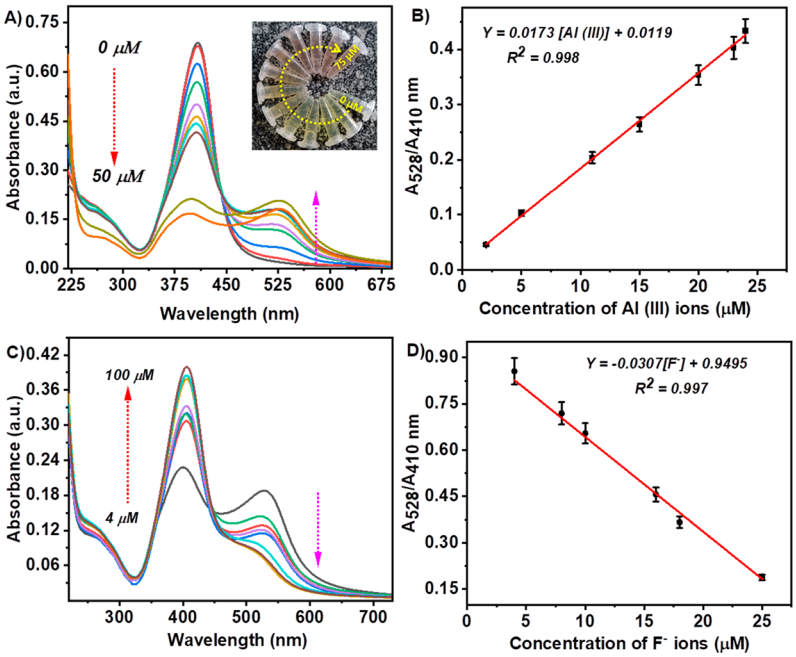

Figure 5. UV−vis absorption spectra and corresponding linear range of the probe in the presence of (A, B) Al(III) ions and (C, D) F^- ions, respectively.

Table 1. Comparison of the Analytical Performance in the Present Work with Some of the Previously Published Colorimetric Al(III) and F^- Ions Sensors

target analyte	probe	linear range	LOD	refs
Al(III)	diaminodiphenyl sulfone@AuNPs	1.0−500 μM	0.62 μM	35
Al(III)	1,2,3-triazole-4,5-dicarboxylic acid@AuNPs	1.5−4.0 μM	0.015 μM	59
Al(III)	ascorbic acid capped@AuNPs	3.7−13 μM	0.46	40
Al(III)	poly(vinylpyrrolidone)@AgNPs	$0.1-10^3$ nM	0.04 μM	60
Al(III)	*N*-lauroyltryramine@AuNPs	1−12 μM	1.15 μM	61
Al(III)	biogenesis@AgNPs	0.05−1 ppm	0.01 ppm	62
Al(III)	tannic acid@AgNPs	2.0−25 μM	0.2 μM	this work
F^-	polyacrylate@AuNPs	30−200 μM	100 μM	39
F^-	thioglucose@AuNPs	20−40 mM	20 mM	37
F^-	AuNPs	120 μM−1.5 mM	120 μM	63
F^-	sulphanilic acid and catechol@AuNPs	1−40 μM	0.2 μM	64
F^-	saponin@AgNPs		10 ppm	65
F^-	3-aminophenylboronic acid and dithiobis(succinimidylpropionate)@AuNPs	75−1000 μM	56.5 μM	66
F^-	4-quinonimine@AuNPs		0.17 μM	67
F^-	tannic acid@AgNPs	4−25 μM	0.19 μM	this work

the absorption intensity at 410 nm accompanied by a visible color change from yellow to red (Figure 4B and Inset). In addition, a new absorption peak appeared at 528 nm (Figure 4B curve-b). Also, after the addition of Al(III) ions, the ζ-potential of TA@AgNPs changed from −19 to −7 mV, which further proved the coordination interaction between TA on the surface of AgNPs and Al(III) ions (Figure S5). Furthermore, the aggregation of TA@AgNPs in the presence of Al(III) ions was proven by TEM images (Figure 4C).

Figure S6 presents the UV−vis absorption spectra of TA@AgNPs in the presence and absence of Al(III) and F^- ions. In the presence of Al(III) ions, TA@AgNPs aggregated (Figure S6, curve-b). However, in the presence of F^- ions (curve-c), the extent of aggregation of TA@AgNPs by Al(III) ions was significantly suppressed. This could be due to the formation of water-soluble strong Al−F complexes[53−55] with the stability constant (βn = 7−19),[56,57] which are significantly higher than those for the Al−TA complexes (βn = 5).[49,57,58] Moreover, as the addition of various concentrations of F^- ions did not cause any significant absorption change in TA@AgNPs (Figure S7), the anti-aggregation effect of F^- ion could be solely due to its interaction with Al(III) ions, which was further proved by the ζ-potential results (Figure S5). The ζ-potentials of TA@AgNPs and TA@AgNPs/Al(III) systems were −19 and −7 mV, respectively. However, in the presence of F^- ions, the ζ-potential result was −15 mV, indicating the anti-aggregation effect of F^- ions. Moreover, the TEM image (Figure 4D) showed well-dispersed TA@AgNPs in the presence of both F^- and Al(III) ions, which further affirmed the antiaggregation effect of F^- ions.

Detection of Al(III) and F^- Ions. The analytical performance of the proposed sensor was evaluated under optimized conditions. As presented in Figure 5A, the absorption of TA@AgNPs at 410 nm gradually and

https://doi.org/10.1021/acsomega.3c05092
ACS Omega 2023, 8, 37293−37301

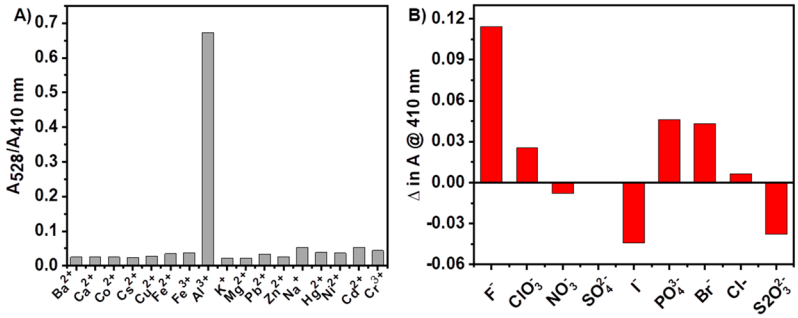

Figure 6. Absorption profile of TA@AgNPs in the presence of (A) various metal ions and (B) various anions in the presence of 30 μM Al(III) ions.

significantly decreased with increasing concentration of Al(III) ions, while the absorption profile at 528 nm showed a gradual increase in a concentration-dependent manner. The aggregation phenomenon can be seen by the naked eye as the color of the test solution gradually changed from yellow to light red with increasing Al(III) ions concentration (Figure 5A, inset). Interestingly, as depicted in Figure 5B, the ratio of change in the absorption (A_{528}/A_{410} nm) can be used to quantitatively detect the concentration of target Al(III) ions. The ratio of change in the absorption showed linearity in the concentration range between 2 and 25 μM. The detection system showed an LOD of 0.2 μM, which is lower than the maximum permissible level of Al(III) ions (7.4 μM) set by WHO for drinking water.

Figure 5C,D presents the analytical performance of the sensor for the detection of F^- ions. As presented in Figure 5C, the absorption profile of the probe at 410 nm increased with an increase in the concentration of F^- ions, while the absorption peak at 528 nm significantly decreased in a concentration-dependent manner. The absorption ratio at 528 and 410 nm showed linearity in the concentration range of 4 to 25 μM. The probe demonstrated an LOD of 0.19 μM, which is lower than that of the higher permissible level of F^- ions (74 μM) set by WHO in drinking water.

Table 1 presents a comparison of the analytical performance of the proposed sensor with those of other methods. As presented in the table, the proposed sensor showed a comparable or superior detection limit. In addition, compared to these methods, the proposed sensing strategy offered a simple, rapid, and sensitive detection procedure and could be used as a potential alternative to conventional methods, which usually involve sophisticated instruments, complicated processes, and a long detection time. Moreover, the proposed sensor employed readily available and biocompatible AgNP functionalizing agents.

Selectivity of the Detection. The applicability of the TA@AgNPs probe for the detection of Al(III) ions in the complex matrix was tested using various possible interfering metal ions. In a particular procedure, the UV−vis absorption response of TA@AgNPs was evaluated in the presence of various metal ions including Ba^{2+}, Ca^{2+}, Co^{2+}, Cs^{2+}, Cu^{2+}, Al^{3+}, Fe^{2+}, Fe^{3+}, K^+, Mg^{2+}, Pb^{2+}, Zn^{2+}, Na^+, Hg^{2+}, Ni^{2+}, Cd^{2+}, and Cr^{3+}. As presented in Figure S8A,B, among the tested metal ions, only Al(III) ions caused significant absorption and color change to the test solution. The absorption ratio A_{528}/A_{410} of Al(III) ions was higher compared to other metal ions (Figure 6A). The result demonstrated the selectivity of the probe for the detection of Al(III) ions. Moreover, compared to various anions, including halogens, only F^- ions successfully prevented the aggregation effect of Al(III) ions on TA@AgNPs (Figures 6B and S8C). The result proved the selectivity of the sensor toward F^- ions.

Real Sample Analysis. The real sample applicability of the sensor was tested using tap water samples collected from Arbaminch University (Ethiopia). Before analysis, the water samples were filtered with a 0.22 μM membrane to remove any suspended particles. Then, the filtered samples were spiked with a series of standard Al(III) or F^- ion solutions, and then the UV−vis absorbance responses were recorded. As presented in Table 2, the samples spiked with Al(III) ions showed a percent recovery between 99 and 102%, with a relative standard deviation (%RSD) less than 5%. Moreover, the samples spiked with F^- ions resulted in a % recovery between 94 and 106% with a %RSD less than 5%. The excellent % recovery and lower %RSD showed the feasibility of the proposed sensor for Al(III) and F^- ions detection in real samples.

Table 2. Application of the Colorimetric Probe for the Detection of Al(III) and F^- Ions in Real Water Samples (n = 3)

method	added (μM)	measured (μM)	recovery (%)	RSD (%)
aluminum	0			
	5	20.31	102	3.2
	10	25.21	100	2.2
	15	34.94	99	0.8
fluoride	0			
	5	4.7	94	2.7
	10	10.4	104	4.4
	15	16.0	106	2.1

CONCLUSIONS

In the present work, we proposed a simple yet sensitive TA@AgNPs-based colorimetric probe for the simultaneous and sensitive detection of Al(III) and F^- ions. The detection procedure was based on the aggregation and anti-aggregation effect of Al(III) and F^- ions, respectively. In the detection system, the chelation between TA with Al(III) ions could cause the aggregation of TA@AgNPs and results in significant absorption and color change. The extent of change in absorption is concentration-dependent and could be used to quantitatively detect target Al(III) ions with an LOD of 0.2 μM. Moreover, in the presence of F^- ions, the aggregation of TA@AgNPs due to the presence of Al(III) ions can be effectively prevented. As a result, F^- ions can be detected based on their anti-aggregation effects, with an LOD of 0.19 μM. Also, the sensor showed excellent applicability for the

https://doi.org/10.1021/acsomega.3c05092
ACS Omega 2023, 8, 37293−37301

detection of Al(III) and F^- ions in real water samples. Moreover, the sensing strategy offered a simple, rapid, and sensitive detection procedure and could be used as a potential alternative to conventional methods, which usually involve sophisticated instruments, complicated processes, and a long detection time. Furthermore, although the as-proposed sensor showed excellent performance, high sensitivity, and selectivity, future work is needed to further boost its sensing performance. In addition, the as-proposed sensor showed a higher response at an acidic pH of 4, which might limit its applicability in biological systems. As a result, a probe with detection capability in a neutral medium needs to be developed (pH = 7). Moreover, it would be necessary to explore a new surface-functionalizing ligand for AgNPs to further improve the stability, selectivity, and sensitivity of the detection system.

■ ASSOCIATED CONTENT

Supporting Information

The Supporting Information is available free of charge at https://pubs.acs.org/doi/10.1021/acsomega.3c05092.

Size distribution histogram of TA@AgNPs (Figure S1); stability of TA@AgNPs at various pH and storage conditions (Figure S2); performance of the probe in various solvents (Figure S3); effect of pH on the probe performance (Figure S4); ζ-potentials (Figure S5); UV−vis absorbance of TA@AgNPs with and without the addition of Al(III) and F^- ions (Figure S6); effect of various F^- ions on the UV−vis absorbance of TA@AgNPs (Figure S7); selectivity of the detection system (Figure S8) (PDF)

■ AUTHOR INFORMATION

Corresponding Author

Terefe Tafese Bezuneh − *Department of Chemistry, College of Natural Sciences, Arbaminch University, 21 Arbaminch, Ethiopia;* orcid.org/0000-0002-2203-6659; Email: teretafe@gmail.com

Authors

Natinael Mekonnen Ofgea − *Department of Chemistry, College of Natural Sciences, Arbaminch University, 21 Arbaminch, Ethiopia;* orcid.org/0000-0002-0485-2476

Solomon Simie Tessema − *Department of Chemistry, College of Natural Sciences, Salale University, 245 Fiche, Ethiopia*

Fuad Abduro Bushira − *Department of Chemistry, College of Natural Sciences, Jima University, 378 Jima, Ethiopia*

Complete contact information is available at: https://pubs.acs.org/10.1021/acsomega.3c05092

Author Contributions

T.T.B.: writing—original draft, investigation, methodology, conceptualization; N.M.O.: performed experiments; S.S.T.: review and writing; F.A.B.: review and writing.

Notes

The authors declare no competing financial interest.

■ ACKNOWLEDGMENTS

The authors acknowledge the Arba Minch University (Ethiopia) for providing research facilities.

■ REFERENCES

(1) Nguyen, T. H. A.; Nguyen, V.-C.; Phan, T. N. H.; Le, V. T.; Vasseghian, Y.; Vasseghian, Y.; Trubitsyn, M. A.; Trubitsyn, M. A.; Nguyen, A.-T.; Nguyen, A. T.; Chau, T. P.; Chau, T. P.; Doan, V.-D. Novel biogenic silver and gold nanoparticles for multifunctional applications: Green synthesis, catalytic and antibacterial activity, and colorimetric detection of Fe (III) ions. *Chemosphere* **2022**, *287*, No. 132271.

(2) ChrisáLe, X. CRISPR/Cas12a-mediated gold nanoparticle aggregation for colorimetric detection of SARS-CoV-2. *Chem. Commun.* **2021**, *57* (56), 6871−6874.

(3) Yu, Y.; Naik, S. S.; Oh, Y.; Theerthagiri, J.; Lee, S. J.; Choi, M. Y. Lignin-mediated green synthesis of functionalized gold nanoparticles via pulsed laser technique for selective colorimetric detection of lead ions in aqueous media. *J. Hazard. Mater.* **2021**, *420*, No. 126585.

(4) Gupta, R.; Kumar, A.; Kumar, S.; Pinnaka, A. K.; Singhal, N. K. Naked eye colorimetric detection of Escherichia coli using aptamer conjugated graphene oxide enclosed Gold nanoparticles. *Sens. Actuators, B* **2021**, *329*, No. 129100.

(5) Saenchoopa, A.; Boonta, W.; Talodthaisong, C.; Srichaiyapol, O.; Patramanon, R.; Kulchat, S. Colorimetric detection of Hg (II) by γ-aminobutyric acid-silver nanoparticles in water and the assessment of antibacterial activities. *Spectrochim. Acta, Part A* **2021**, *251*, No. 119433.

(6) Balasurya, S.; Syed, A.; Thomas, A. M.; Marraiki, N.; Elgorban, A. M.; Raju, L. L.; Das, A.; Khan, S. S. Rapid colorimetric detection of mercury using silver nanoparticles in the presence of methionine. *Spectrochim. Acta, Part A* **2020**, *228*, No. 117712.

(7) Mao, L.; Wang, Q.; Luo, Y.; Gao, Y. Detection of Ag+ ions via an anti-aggregation mechanism using unmodified gold nanoparticles in the presence of thiamazole. *Talanta* **2021**, *222*, No. 121506.

(8) Fan, P.; He, S.; Cheng, J.; Hu, C.; Liu, C.; Yang, S.; Liu, J. l-Cysteine modified silver nanoparticles-based colorimetric sensing for the sensitive determination of Hg2+ in aqueous solutions. *Luminescence* **2021**, *36* (3), 698−704.

(9) Maruthupandi, M.; Vasimalai, N. Nanomolar detection of L-cysteine and Cu2+ ions based on Trehalose capped silver nanoparticles. *Microchem. J.* **2021**, *161*, No. 105782.

(10) Zhang, Y.; Huang, Y.; Fu, L.; Qiu, J.; Wang, Z.; Wu, A. Colorimetric detection of paraquat in aqueous and fruit juice samples based on functionalized gold nanoparticles. *J. Food Compos. Anal.* **2020**, *92*, No. 103574.

(11) Rujiralai, T.; Cheewasedtham, W.; Jayeoye, T. J.; Kaewsara, S.; Plaisen, S. Hydrolyzed product mediated aggregation of l-cysteine-modified gold nanoparticles as a colorimetric probe for carbamate residues in chilis. *Anal. Lett.* **2020**, *53* (4), 574−588.

(12) Mousavizadeh, F. S.; Sarlak, N. A sensitive dual mode turn-on fluorescence and colorimetric nanosensor for ultrasensitive detection of trace amount of gluten proteins in bread products based on crystalline nano cellulose and gold nanoparticles. *Spectrochim. Acta, Part A* **2023**, *287*, No. 122095.

(13) Ul Haq, M. A.; Hussain, K.; Aslam, Z.; Umar, A. R.; Shah, M. R.; Sirajuddin; Ur-Rehman, M.; Sherazi, S. T. H.; Nisar, J. Highly selective sub-micromolar level colorimetric sensor for lanthanum detection based on l-tyrosine functionalized silver nanoparticles. *Microchem. J.* **2023**, *185*, No. 108289.

(14) Rasheed, S.; Ahmad, N.; ul Haq, M. A.; Ahmad, W.; Hussain, D.; Sirajuddin Dual-mode highly selective colorimetric and smartphone-based paper sensors utilizing silver nanoparticles for ultra-trace level omeprazole detection in complex matrices *J. Ind. Eng. Chem.* **2023** DOI: 10.1016/j.jiec.2023.08.009.

(15) Tarighat, M. A.; Ghorghosheh, F. H.; Abdi, G. Fe3O4@SiO2-Ag nanocomposite colorimetric sensor for determination of arginine and ascorbic acid based on synthesized small size AgNPs by cystoseria algae extract. *Mater. Sci. Eng.: B* **2022**, *283*, No. 115855.

(16) Yuan, K.; Sun, Y.; Liang, F.; Pan, F.; Hu, M.; Hua, F.; Yuan, Y.; Nie, J.; Zhang, Y. Tyndall-effect-based colorimetric assay with colloidal silver nanoparticles for quantitative point-of-care detection

of creatinine using a laser pointer pen and a smartphone. *RSC Adv.* **2022**, *12* (36), 23379−23386.
(17) Ali, S.; Umar, A. R.; Hussain, K.; Muhammad, H.; Hanif, M.; Laiche, M. H.; Rasheed, S.; Yasmeen, K.; Hameed, A.; Shah, M. R. Ultra-trace level colorimetric composite sensor based on novel DH-1,6-NAPY-8-CN-AgNPs for the detection of Clonazepam in aqueous and human plasma samples. *J. Ind. Eng. Chem.* **2023**, *125*, 136−143.
(18) Liu, G.; Lu, M.; Huang, X.; Li, T.; Xu, D. Application of Gold-Nanoparticle Colorimetric Sensing to Rapid Food Safety Screening. *Sensors* **2018**, *18* (12), No. 4166.
(19) Shellaiah, M.; Sun, K.-W. Review on Anti-Aggregation-Enabled Colorimetric Sensing Applications of Gold and Silver Nanoparticles. *Chemosensors* **2022**, *10* (12), No. 536.
(20) Liu, B.; Zhuang, J.; Wei, G. Recent advances in the design of colorimetric sensors for environmental monitoring. *Environ. Sci.: Nano* **2020**, *7* (8), 2195−2213.
(21) Zhao, W.; Brook, M. A.; Li, Y. Design of gold nanoparticle-based colorimetric biosensing assays. *ChemBioChem* **2008**, *9* (15), 2363−2371.
(22) Daniel, M.-C.; Astruc, D. Gold nanoparticles: assembly, supramolecular chemistry, quantum-size-related properties, and applications toward biology, catalysis, and nanotechnology. *Chem. Rev.* **2004**, *104* (1), 293−346.
(23) Ghosh, S. K.; Pal, T. Interparticle Coupling Effect on the Surface Plasmon Resonance of Gold Nanoparticles: From Theory to Applications. *Chem. Rev.* **2007**, *107* (11), 4797−4862.
(24) Delhaize, E.; Ryan, P. R. Aluminum toxicity and tolerance in plants. *Plant Physiol.* **1995**, *107* (2), 315−321.
(25) Greger, J. L.; Sutherland, J. E.; Yokel, R. Aluminum exposure and metabolism. *Crit. Rev. Clin. Lab. Sci.* **1997**, *34* (5), 439−474.
(26) Ma, Y.-H.; Yuan, R.; Chai, Y.-Q.; Liu, X.-L. A new aluminum (III)-selective potentiometric sensor based on N, N′-propanediamide bis (2-salicylideneimine) as a neutral carrier. *Mater. Sci. Eng.: C* **2010**, *30* (1), 209−213.
(27) Sorenson, J. R. J.; Campbell, I. R.; Tepper, L. B.; Lingg, R. D. Aluminum in the environment and human health. *Environ. Health Perspect.* **1974**, *8*, 3−95.
(28) Kaur, K.; Bhardwaj, V. K.; Kaur, N.; Singh, N. Imine linked fluorescent chemosensor for Al3+ and resultant complex as a chemosensor for HSO4− anion. *Inorg. Chem. Commun.* **2012**, *18*, 79−82.
(29) Liao, Z.-C.; Yang, Z.-Y.; Li, Y.; Wang, B.-D.; Zhou, Q.-X. A simple structure fluorescent chemosensor for high selectivity and sensitivity of aluminum ions. *Dyes Pigm.* **2013**, *97* (1), 124−128.
(30) Graves, A. B.; White, E.; Koepsell, T. D.; Reifler, B. V.; van Belle, G.; Larson, E. B. The association between aluminum-containing products and Alzheimer's disease. *J. Clin. Epidemiol.* **1990**, *43* (1), 35−44.
(31) Perl, D. P.; Gajdusek, D. C.; Garruto, R. M.; Yanagihara, R. T.; Gibbs, C. J. Intraneuronal aluminum accumulation in amyotrophic lateral sclerosis and parkinsonism-dementia of Guam. *Science* **1982**, *217* (4564), 1053−1055.
(32) Mukhopadhyay, A.; Maka, V. K.; Moorthy, J. N. Fluoride-triggered ring-opening of photochromic diarylpyrans into merocyanine dyes: Naked-eye sensing in subppm levels. *J. Org. Chem.* **2016**, *81* (17), 7741−7750.
(33) Cametti, M.; Rissanen, K. Highlights on contemporary recognition and sensing of fluoride anion in solution and in the solid state. *Chem. Soc. Rev.* **2013**, *42* (5), 2016−2038.
(34) Wade, C. R.; Broomsgrove, A. E.; Aldridge, S.; Gabbai, F. P. Fluoride ion complexation and sensing using organoboron compounds. *Chem. Rev.* **2010**, *110* (7), 3958−3984.
(35) Meena, R.; Mehta, V. N.; Bhamore, J. R.; Rao, P. T.; Park, T.-J.; Kailasa, S. K. Diaminodiphenyl sulfone as a novel ligand for synthesis of gold nanoparticles for simultaneous colorimetric assay of three trivalent metal cations (Al3+, Fe3+ and Cr3+). *J. Mol. Liq.* **2020**, *312*, No. 113409.
(36) Garg, N.; Bera, S.; Ballal, A. SPR responsive xylenol orange functionalized gold nanoparticles- optical sensor for estimation of Al3+ in water. *Spectrochim. Acta, Part A* **2020**, *228*, No. 117701.
(37) Watanabe, S.; Seguchi, H.; Yoshida, K.; Kifune, K.; Tadaki, T.; Shiozaki, H. Colorimetric detection of fluoride ion in an aqueous solution using a thioglucose-capped gold nanoparticle. *Tetrahedron Lett.* **2005**, *46* (51), 8827−8829.
(38) Zhu, R.; Song, J.; Ma, Q.; Zhou, Y.; Yang, J.; Shuang, S.; Dong, C. A colorimetric probe for the detection of aluminum ions based on 11-mercaptoundecanoic acid functionalized gold nanoparticles. *Anal. Methods* **2016**, *8* (39), 7232−7236.
(39) Kumar, A.; Bhatt, M.; Vyas, G.; Bhatt, S.; Paul, P. Sunlight Induced Preparation of Functionalized Gold Nanoparticles as Recyclable Colorimetric Dual Sensor for Aluminum and Fluoride in Water. *ACS Appl. Mater. Interfaces* **2017**, *9* (20), 17359−17368.
(40) Rastogi, L.; Dash, K.; Ballal, A. Selective colorimetric/visual detection of Al3+ in ground water using ascorbic acid capped gold nanoparticles. *Sens. Actuators, B* **2017**, *248*, 124−132.
(41) Ranoszek-Soliwoda, K.; Tomaszewska, E.; Socha, E.; Krzyczmonik, P.; Ignaczak, A.; Orlowski, P.; Krzyzowska, M.; Celichowski, G.; Grobelny, J. The role of tannic acid and sodium citrate in the synthesis of silver nanoparticles. *J. Nanopart. Res.* **2017**, *19* (8), No. 273.
(42) Yi, Z.; Li, X.; Xu, X.; Luo, B.; Luo, J.; Wu, W.; Yi, Y.; Tang, Y. Green, effective chemical route for the synthesis of silver nanoplates in tannic acid aqueous solution. *Colloids Surf., A* **2011**, *392* (1), 131−136.
(43) Huang, X.; Wu, H.; Pu, S.; Zhang, W.; Liao, X.; Shi, B. One-step room-temperature synthesis of Au@Pd core−shell nanoparticles with tunable structure using plant tannin as reductant and stabilizer. *Green Chem.* **2011**, *13* (4), 950−957.
(44) Bastús, N. G.; Merkoçi, F.; Piella, J.; Puntes, V. Synthesis of highly monodisperse citrate-stabilized silver nanoparticles of up to 200 nm: kinetic control and catalytic properties. *Chem. Mater.* **2014**, *26* (9), 2836−2846.
(45) Cao, Y.; Zheng, R.; Ji, X.; Liu, H.; Xie, R.; Yang, W. Syntheses and Characterization of Nearly Monodispersed, Size-Tunable Silver Nanoparticles over a Wide Size Range of 7−200 nm by Tannic Acid Reduction. *Langmuir* **2014**, *30* (13), 3876−3882.
(46) Gangwar, C.; Yaseen, B.; Kumar, I.; Singh, N. K.; Naik, R. M. Growth Kinetic Study of Tannic Acid Mediated Monodispersed Silver Nanoparticles Synthesized by Chemical Reduction Method and Its Characterization. *ACS Omega* **2021**, *6* (34), 22344−22356.
(47) Guo, J.; Ping, Y.; Ejima, H.; Alt, K.; Meissner, M.; Richardson, J. J.; Yan, Y.; Peter, K.; Von Elverfeldt, D.; Hagemeyer, C. E. Engineering multifunctional capsules through the assembly of metal−phenolic networks. *Angew. Chem., Int. Ed.* **2014**, *53* (22), 5546−5551.
(48) Krywko-Cendrowska, A.; Marot, L.; Mathys, D.; Boulmedais, F. Ion-Imprinted Nanofilms Based on Tannic Acid and Silver Nanoparticles for Sensing of Al(III). *ACS Appl. Nano Mater.* **2021**, *4* (5), 5372−5382.
(49) Zhang, L.; Liu, R.; Gung, B. W.; Tindall, S.; Gonzalez, J. M.; Halvorson, J. J.; Hagerman, A. E. Polyphenol−aluminum complex formation: implications for aluminum tolerance in plants. *J. Agric. Food. Chem.* **2016**, *64* (15), 3025−3033.
(50) Espina, A.; Cañamares, M. V.; Jurašeková, Z.; Sanchez-Cortes, S. Analysis of Iron Complexes of Tannic Acid and Other Related Polyphenols as Revealed by Spectroscopic Techniques: Implications in the Identification and Characterization of Iron Gall Inks in Historical Manuscripts. *ACS Omega* **2022**, *7* (32), 27937−27949.
(51) Falcão, L.; Araújo, M. E. M. Vegetable tannins used in the manufacture of historic leathers. *Molecules* **2018**, *23* (5), No. 1081.
(52) Ricci, A.; Olejar, K. J.; Parpinello, G. P.; Kilmartin, P. A.; Versari, A. Application of Fourier transform infrared (FTIR) spectroscopy in the characterization of tannins. *Appl. Spectrosc. Rev.* **2015**, *50* (5), 407−442.
(53) Ahmad, M.; Narayanaswamy, R. Fibre optic reflectance sensor for the determination of aluminium (III) in aqueous environment. *Anal. Chim. Acta* **1994**, *291* (3), 255−260.

https://doi.org/10.1021/acsomega.3c05092
ACS Omega 2023, 8, 37293−37301

(54) El-Wekil, M. M.; Ali, H. R. H.; Marzouk, A. A.; Ali, R. Synthesis of Fe 3 O 4 nanobead-functionalized 8-hydroxyquinoline sulfonic acid supported by an ion-imprinted biopolymer as a recognition site for Al 3+ ions: estimation in human serum and water samples. *New J. Chem.* **2018**, *42* (12), 9828−9836.
(55) Ng, S. M.; Narayanaswamy, R. Fluorescence sensor using a molecularly imprinted polymer as a recognition receptor for the detection of aluminium ions in aqueous media. *Anal. Bioanal. Chem.* **2006**, *386*, 1235−1244.
(56) Rydzek, G.; Schaaf, P.; Voegel, J.-C.; Jierry, L.; Boulmedais, F. Strategies for covalently reticulated polymer multilayers. *Soft Matter* **2012**, *8* (38), 9738−9755.
(57) Krywko-Cendrowska, A.; Marot, L.; Mathys, D.; Boulmedais, F. Ion-imprinted nanofilms based on tannic acid and silver nanoparticles for sensing of Al (III). *ACS Appl. Nano Mater.* **2021**, *4* (5), 5372−5382.
(58) Barquero, M.; Dominguez, O.; Alonso, M.; Arcos, M. Biosensor for aluminum (III) based on a-chymotrypsin inhibition using a disposable screen-printed carbon electrode and acetyl-tyrosine ethyl ester as substrate. *Chem. Sci. J.* **2015**, *6*, No. 89.
(59) Zhao, S.; Chen, L.; Liu, F.; Fan, Y.; Liu, Y.; Han, Y.; Hu, Y.; Su, J.; Song, C. Rapid and selective detection of aluminum ion using 1,2,3-triazole-4,5-dicarboxylic acid-functionalized gold nanoparticle-based colorimetric sensor. *RSC Adv.* **2021**, *11* (49), 30635−30645.
(60) del Portal-Vázquez, P. R.; López-Pérez, G.; Prado-Gotor, R.; Román-Hidalgo, C.; Martín-Valero, M. J. Citrate and Polyvinylpyrrolidone Stabilized Silver Nanoparticles as Selective Colorimetric Sensor for Aluminum (III) Ions in Real Water Samples. *Materials* **2020**, *13* (6), No. 1373.
(61) Megarajan, S.; Veerappan, A. A selective pink-to-purple colorimetric sensor for aluminium via the aggregation of gold nanoparticles. *Opt. Mater.* **2020**, *108*, No. 110177.
(62) Joshi, P.; Nemiwal, M.; Al-Kahtani, A. A.; Ubaidullah, M.; Kumar, D. Biogenic AgNPs for the non-cross-linking detection of aluminum in aqueous systems. *J. King Saud Univ., Sci.* **2021**, *33* (6), No. 101527.
(63) Gu, J.-A.; Lin, Y.-J.; Chia, Y.-M.; Lin, H.-Y.; Huang, S.-T. Colorimetric and bare-eye determination of fluoride using gold nanoparticle agglomeration probes. *Microchim. Acta* **2013**, *180* (9), 801−806.
(64) Motahhari, A.; Abdolmohammad-Zadeh, H.; Farhadi, K. Development of a New Fluoride Colorimetric Sensor Based on Anti-aggregation of Modified Silver Nanoparticles. *Anal. Bioanal. Chem. Res.* **2021**, *8* (1), 79−89.
(65) Debnath, B.; Das, R. Presence of fluoride in water diminishes fast the SPR peak of silver nanocrystals showing large red shift with quick sedimentation − A fast sensing and fast removal case. *Spectrochim. Acta, Part A* **2021**, *249*, No. 119306.
(66) Jayeoye, T. J.; Rujiralai, T. Sensitive and selective colorimetric probe for fluoride detection based on the interaction between 3-aminophenylboronic acid and dithiobis(succinimidylpropionate) modified gold nanoparticles. *New J. Chem.* **2020**, *44* (15), 5711−5719.
(67) Kundu, S.; Kar, P. Selective Colorimetric Sensing of Fluoride Ion in Water by 4-Quinonimine Functionalized Gold Nanoparticles. *J. Cluster Sci.* **2023**, 1−11.

https://doi.org/10.1021/acsomega.3c05092
ACS Omega 2023, 8, 37293−37301